Atom Indonesia

Journal homepage: http://aij.batan.go.id

Optimizing Neutronic and Photonic Performance in Irradiation Systems of Symmetric TRIGA Cores

S. M. Shauddin

Institute of Nuclear Science and Technology, Atomic Energy Research Establishment, Ganakbari, Savar, Dhaka-1349, Bangladesh

ARTICLE INFO

Article history:
Received 24 February 2022
Received in revised form 19 February 2023
Accepted 30 March 2023

Keywords:

Beam-port
Thermal neutron flux
Gamma photon flux
Irradiation system
TRIGA
MCNP

ABSTRACT

The BAEC TRIGA MARK-II Research Reactor (BTRR) in Bangladesh has been used for a wide range of purposes, including basic and applied nuclear research and human resource development. Therefore, its core management should be flexible to meet various objectives with different priorities and to deliver the best possible outcome. In this study, neutron and gamma photon flux variation was studied at different radial and axial irradiation systems of the current core (C-0) as well as six symmetric reconfigurations (C-1, C-2, C-3, C-4, C-5, and C-6) of the existing BTRR using the universal MCNP code. While keeping the exact core component and material density, the symmetric reconfigured cores were modeled based on core criticality calculation and excess reactivity in the critical state. Finally, it was observed that the reconfigured core C-1 has the best neutronic and photonic performance at the irradiation systems compared to other reconfigured cores, against the reference core C-0.

INTRODUCTION

BAEC (Bangladesh Atomic Energy Commission) TRIGA MARK-II Research Reactor (BTRR) has been efficiently used in various fields of fundamental nuclear research, human resource development, and production of radio-isotopes since 1986. It is a light water cooled and graphite reflected pool-type reactor designed for steady-state and square-wave operation up to a thermal power level of 3 MW and for pulsing mode with the highest power level of 852 MW [1]. One hundred standard low enriched uranium (LEU) type fuel elements are assembled in the reactor core. Fuel element (FE) consists of 20 wt% Uranium enriched to about 19.7 wt% of U-235, Zirconium Hydride ($ZrH_{1.6}$) and 0.47 wt% Erbium (Er). The reactivity of the reactor is controlled by five fuel follower and one air follower control rods which contain Boron Carbide (B_4C) as the neutron absorber material. The central neutron flux is suppressed by eighteen graphite dummy elements located around the center (13) and near the periphery (5). In order to support its research and development (R&D) purpose, the TRIGA Mark-II research reactor is equipped with a number of radial/horizontal and axial/vertical in-core and ex-core irradiation facilities. The vertical irradiation facilities are (i) Dry Central Thimble (DCT) and (ii) Pneumatic Transfer System (PTS). In the DCT, samples may be exposed to an average thermal neutron flux density of 7.46E+13 n/cm^2.s. It is used mainly for radioisotope production. The PTS is also called the Rabbit system, where the average thermal neutron flux is 1.0E+13 n/cm^2.s. It is used for the production of very short-lived radioisotopes. On the other hand, the horizontal irradiation facilities are furnished with Thermal Column and four neutron beam tubes: Tangential Beam Tube (TBT), Piercing Beam Tube (PBT), Radial Beam Tube (RBT)-I, and Radial Beam Tube (RBT)-II. The thermal column facility filled with heavy concrete blocks is not yet used. The average thermal neutron flux in each type of beam port is 7.5E+10 n/cm^2.s. The TBT is used for neutron radiography analysis and the PBT is used for neutron scattering studies by using Triple Axes Spectrometer (TAS).

Recently, studies based on the measurement (by experiment) or computation (by code) of neutron and photon flux in the irradiation systems of the core

*Corresponding author.
E-mail address: smshauddin@yahoo.com
DOI: https://doi.org/10.55981/aij.2023.1219

and outside the core have been carried out for several specific purposes. Aljaž Kolšek et. al. designed an irradiation device inside the JSI TRIGA Mark-II research reactor that irradiates with thermal neutrons [2]. Damien Fourmentel et. al., completed a combined analysis of neutron and photon flux measurements for the Jules Horowitz Reactor core mapping [3]. Neutron flux measurements were carried out by Davide Chiesa et. al. at two irradiation facilities of the TRIGA Mark II reactor at ENEA Casaccia Research Center, Italy, for radiation damage tests [4]. Presently, a day neutron activation technique is widely used for measuring neutron and gamma photonic flux at the beam ports of the TRIGA research reactor [5-7]. The aim of this study is not only to calculate the flux at the beam ports with probabilistic approach but also to discover a more optimum TRIGA core configuration for better irradiation system than the existing core. Core performance has been optimized using various neutronic and photonic calculations, comparisons and analyses to radial and axial irradiation systems based on the Monte Carlo method. While keeping exact elemental geometry, material composition, and density of the present core, six symmetric different configurations of the TRIGA core have been designed.

METHODOLOGY

The MCNP model of the TRIGA reactor reference core consists of one hundred standard FE, six control rods (located in D-ring), eighteen GDEs, one DCT (located in A-ring) and one PTS irradiation terminus (located in F-ring). All these elements are placed and supported in-between top and bottom grid plate and arranged in 7 hexagonal rings A, B, C, D, E, F and G of a hexagonal lattice as shown in Fig. 1. The MCNP reference core model has been validated by benchmarking the neutronic parameters with the experimental, calculation and Safety Analysis Report (SAR) in the earlier study [8]. In this study, core neutronic and photonic characteristics at the different irradiation systems have been analyzed for the reference (C-0) and six symmetric reconfigured TRIGA cores (C-1, C-2, C-3, C-4, C-5, and C-6) each having the same number of fuel element (FE), graphite dummy elements (GDE) and other components. To avoid loss in excess reactivity, FE and GDE were maintained the same as the original in reconfigured cores. The reconfiguration was performed by maintaining two factors: (i) replacement between FE and GDE, and (ii) core's sub-criticality value (when all control rods are fully inserted into the active core) [8].

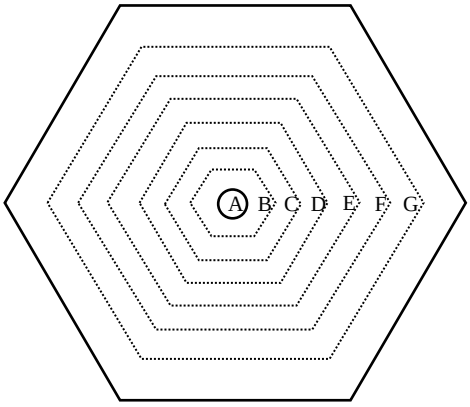

Fig. 1. Hexagonal rings in a hexagonal lattice of the TRIGA core.

In this MCNP TRIGA core models, the reactor core geometry which covers all fuel rods (fuel, clad and gap), control rods, grid plate, graphite reflector, beam tubes, and Lazy Susan (rotary specimen rack) is considered carefully. In the Monte Carlo simulation, the first 100 cycles were skipped, followed by 1000 active cycles with 20,000 particles per cycle. The temperature was maintained to be 27 °C for the density and cross-section data of all materials. In this study, the calculation was done with the Monte Carlo code MCNP5 [9] using the cross section library based on ENDF/B-VII [10]. Track length estimate of neutron flux was calculated using tally type F4 [11]. S(α,β) scattering cross sections option were used for Zirconium hydride ($ZrH_{1.6}$), light water (H_2O) and graphite (C). All the calculations were completed for fresh core i.e. zero burnup condition. Beam ports are characterized by calculating the thermal (up to 0.625 eV) neutron flux, thermal to higher (>0.625 eV) neutron flux ratio and with photon flux (up to 20 MeV). Neutron flux was estimated at the end position of graphite reflector, i.e. at the end of tangential, piercing and radial beam port. All material and geometric data are incorporated from the manufacture and consignment documentation, provided by the reactor manufacturer General Atomics of USA [1]. The reference (C-0) and the reconfigured (C-1, C-2, C-3, C-4, C-5 and C-6) cores of the TRIGA reactor including their axial/vertical irradiation systems (DCT and PTS) are shown in Fig. 2. Lazy Susan and the radial/horizontal irradiation systems of the reference core are depicted in Fig. 3.

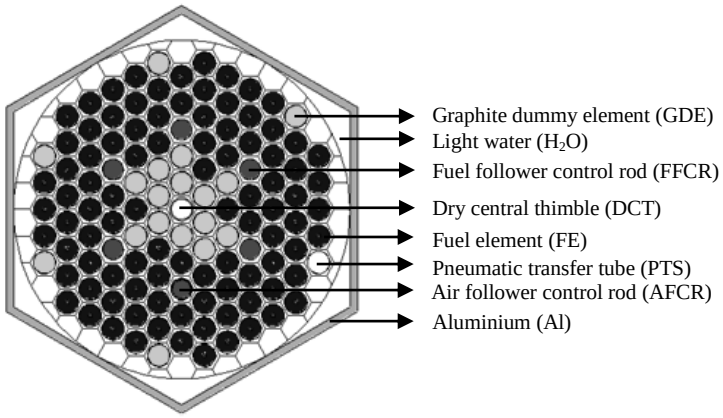

Reference core (C-0)

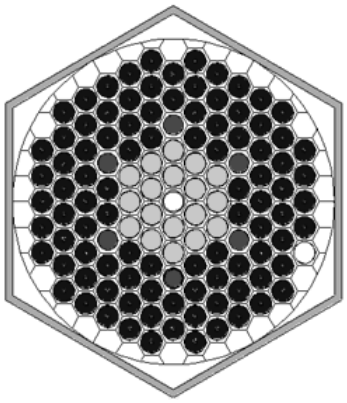

C-1

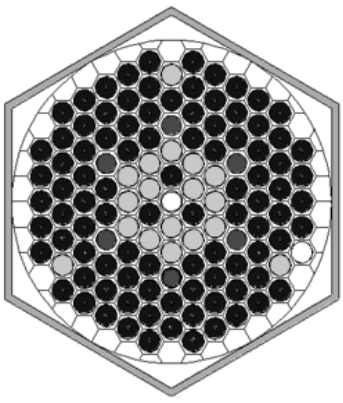

C-2

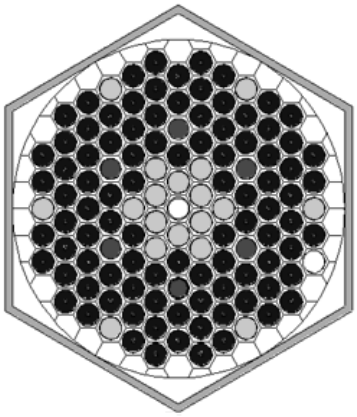

C-3

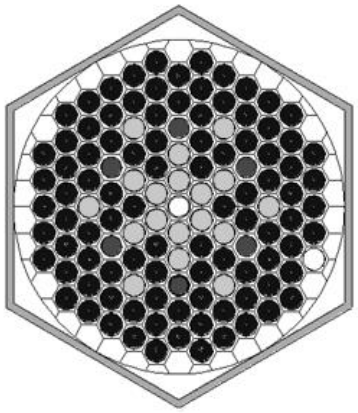

C-4

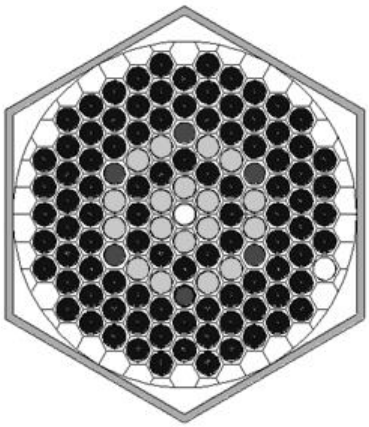

C-5

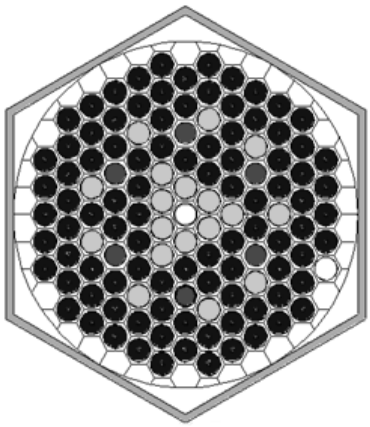

C-6

Fig. 2. Reference and reconfigured (R&R) cores of the TRIGA MARK II research reactor.

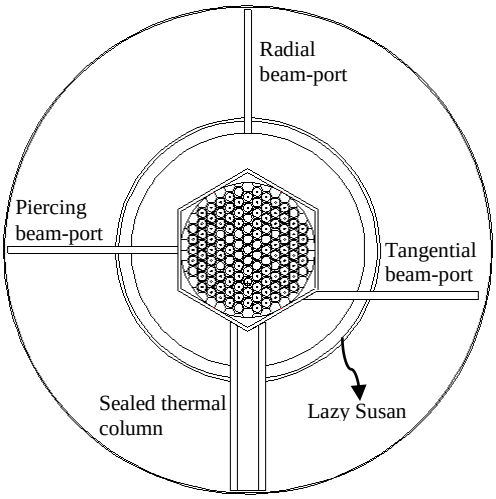

Fig. 3. MCNP TRIGA core model with horizontal irradiation facilities.

RESULTS AND DISCUSSION

Criticality calculation

Core criticality calculation is very important for not only reactor design but also nuclear safety during operation. Effective multiplication factor (k_{eff}) values of the reference and reconfigured (R&R) cores have been calculated at core subcritical and supercritical state. The k_{eff} results and fission detected thermal to higher energy neutron ratio of the R&R cores are nicely presented in Fig. 4. Here the subcritical (all control rods are fully inserted) and supercritical (all control rods are fully withdrawn) state of the core is indicated by the symbol ↓ and ↑ respectively. It is seen that the reconfigured core C-1 & C-6 has the lowest and the highest k_{eff} value at core subcritical and supercritical state, respectively. The reconfigured core C-1 & C-6 have almost 1.84 % less and 0.22 % more k_{eff} value comparable to that of the reference core at core subcritical and supercritical state. On the other hand, the reconfigured core C-5 has the highest value of thermal to higher energy neutron ratio. The reconfigured core C-4, C-5, and C-6 are better to compare to that of the reference core when only the detected thermal fission neutron is considered in core design. However, the reconfigured core C-1 is compared to that of the reference core when only the shutdown margin is considered in core safety. When both parameters are considered in core design and safety, the reconfigured core C-3 is better compared to that of the reference core.

The thermal neutron flux and detected thermal fission to higher energy neutron ratio of the R&R cores at critical state are shown in Fig. 5. It is observed that although the reconfigured core C-2, C-4, C-5, and C-6 have relatively higher detected thermal fission neutrons at 300 K, they have lower thermal flux compare to that of the other cores. The reconfigured core C-1 and C-3 show comparatively higher thermal neutron flux as the reference core C-0. Moreover, it is concluded that the reconfigured core C-1 performs better in producing more thermal neutron flux compared to the reference core. It is known that neutron thermalization rate depends on the moderating ratio. It is the ratio of Macroscopic Slowing Down Power (MSDP) and macroscopic absorption cross-section. H_2O has comparatively higher MSDP among the moderators. However, its moderating ratio is low due to its relatively higher absorption cross-section**.** On the other hand, despite being a heavier nucleus, graphite has much lower MSDP. It is a better moderator than H_2O due to its lower absorption cross-section than H_2O. Due to a combined thermal flux of the moderator/coolant (H_2O) and compact GDEs (graphite) around the DCT the core C-1 and C-3 show the higher thermal flux than the reference core.

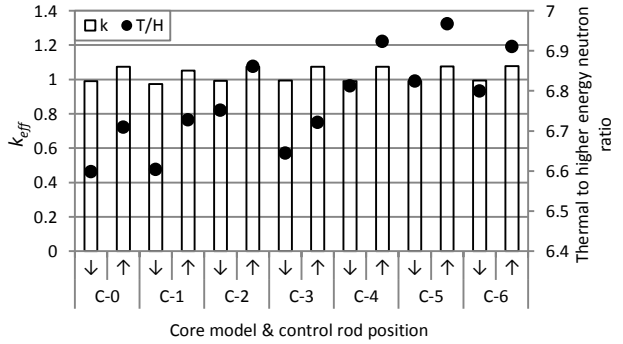

Fig. 4. k_{eff} & thermal to higher energy neutron ratio of the R&R cores at subcritical and supercritical state.

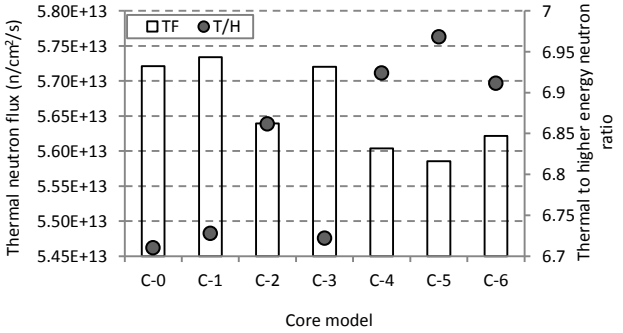

Fig. 5. Thermal neutron flux & thermal to higher energy neutron ratio of the R&R cores at critical state.

Excess reactivity is one of the crucial parameters for nuclear reactor design and safety. The excess reactivity of the R&R cores at critical state is presented in Table 1. The uncertainty is calculated from the standard statistical formula of error propagation using the 1 standard deviation estimates for k_{eff}**.** In the excess reactivity calculations, it is seen that the reconfigured core C-1 has the lowest excess reactivity compare to that of the other cores. The core C-1 has around 21 %

smaller excess reactivity compared to the reference core. Meanwhile, core C-3, C-4, and C-5 show about 8 % more excess reactivity compared to the reference core. The reference core C-0 and the reconfigured core C-2 show the next lowest excess reactivity, respectively. The other cores show approximately the same excess reactivity.

Table. 1. Excess reactivity of the R&R cores at critical state.

Core model	k_{eff} ±Δ* (critical)	Excess reactivity ($±Δ^{\#}$)
C-0	1.00058±0.00019	10.08000±0.10083
C-1	1.00046±0.00018	7.989230±0.09907
C-2	1.00034±0.00018	10.67846±0.09995
C-3	0.99972±0.00019	10.94000±0.09863
C-4	1.00016±0.00018	10.94462±0.09684
C-5	1.00005±0.00018	10.86000±0.09774
C-6	0.99967±0.00019	10.99385±0.09910

*The statistical uncertainity is shown for one standard deviation.

Neutron flux at horizontal beam-ports

In order to get good irradiation service from the research reactor, it is, therefore, necessary to know the distribution of relative thermal flux at the end of horizontal beam-ports such as piercing, tangential, and radial. In this study, the relative distributions of thermal flux in the beam-ports have been calculated with associated standard deviation. The results have been compared with the previous work done by the approximately same TRIGA core [12]. Table 2 and Table 3 respectively represent the geometry, static and kinetic parameters differences, and the variations in the results (thermal neutron and gamma photon flux) between two models. It is observed that the order of the thermal neutron flux of the two studies is the same, with the exception of RBP as the value is slightly higher in the present study than in the previous work. This is due to the fact that there is more moderator/coolant area in this study for neutron thermalization. By contrast, the gamma photon flux of the previous study is higher than that of the present study. The reason behind this scenario is the perfect absorber boundary condition had been considered surrounding the whole core of the previous work. Figure 6 depicts the relative distribution of thermal flux in the horizontal beam-ports and thermal to higher energy neutron flux ratio of the R&R TRIGA cores. According to placement and connectivity with core, different beam-ports of a core gain different thermal flux. Moreover, thermal flux in a beam-port of reconfigured core is found to vary significantly from one core to another. The reason behind the scenario is the reconfiguration of the TRIGA core through substitution between FEs and GDEs. The main function of GDE is to moderate the excess flux in the core. If the inner part of a beam-port encounters more GDEs across the core, then it achieves lower thermal flux than the beam-port that encounters less GDEs. It is seen that the PBP and TBP of all the reconfigured cores have higher thermal to higher neutron flux ratio compare to that of the reference core. However, thermal to higher neutron flux ratio of RBP varies considerably from one core to another. The reconfigured core C-1 represents the best performance compared to the reference and other reconfigured cores providing the maximum thermal neutron flux to all the horizontal beam ports (Table 4).

Table. 2. Geometry, static & kinetic parameters differences between two models.

Parameters	Present study (Existing model)	Previous study [12]
Number of Fuel element	95	127
DCT, PTS, FFCR, AFCR & GDE	Exist	Not exist
Reflector surrounding the core	C, Pb, Al & H_2O	C
k_{eff} (without control rod)	1.07483	1.18300
β-eff	0.00704	0.00688
ℓ_p (μs)	33.5	94.5

Table. 3. Thermal neutron and gamma photon flux differences between two models.

Beam port	Flux	Present study	Previous study [12]
PBP	n	4.15248E-04±7.88971E-06	1.550E-04±6.386E-06
	p	5.20899E-04±1.20849E-05	1.728E-03±4.285E-05
TBP	n	4.72330E-04±7.88971E-06	1.525E-04±6.253E-06
	p	4.90896E-04±1.16342E-05	1.143E-03±3.372E-05
RBP	n	2.13844E-04±5.45302E-06	3.853E-05±3.202E-06
	p	2.27777E-04±7.24331E-06	3.356E-04±1.769E-05

Table. 4. Comparison of optimum neutron and photon flux at the irradiation systems of the R&R cores.

Irradiation system	Flux	1st Optimum core	2nd optimum core	1st optimum core value	2nd optimum core value	Reference core value
PBP	n	C-1	C-4	4.90934E-04 ±8.83681E-06	4.62560E-04 ±8.55736E-06	4.15248E-04 ±7.88971E-06
	p	C-5	C-6	6.22090E-04 ±9.82902E-06	6.08422E-04 ±9.73475E-06	5.20899E-04 ±1.20849E-05
TBP	n	C-1	C-0	4.77950E-04 ±8.98546E-06	4.72330E-04 ±7.88971E-06	4.72330E-04 ±7.88971E-06
	p	C-6	C-3	5.59605E-04 ±9.84905E-06	5.55851E-04 ±9.89415E-06	4.90896E-04 ±1.16342E-05
RBP	n	C-1	C-5	2.52931E-04 ±6.04505E-06	2.40300E-04 ±5.91138E-06	2.13844E-04 ±5.45302E-06
	p	C-5	C-3	2.85913E-04 ±6.60459E-06	2.82365E-04 ±6.52263E-06	2.27777E-04 ±7.24331E-06
LS	n	C-1	C-4	9.53091E-02 ±1.52495E-04	9.07742E-02 ±1.54316E-04	8.85189E-02 ±1.50482E-04
	p	C-1	C-2	2.65306E-01 ±3.18367E-04	2.57433E-01 ±3.08920E-04	2.53698E-01 ±3.29807E-04
DCT	n	C-1	C-2	7.26611E-02 ±2.03451E-04	7.19524E-02 ±2.30248E-04	6.68736E-02 ±1.93933E-04
	p	C-2	C-0	1.46268E-01 ±3.21790E-04	1.45440E-01 ±3.19968E-04	1.45440E-01 ±3.19968E-04
PTS	n	C-2	C-0	2.92399E-02 ±1.37428E-04	2.73081E-02 ±1.31079E-04	2.73081E-02 ±1.31079E-04
	p	C-0	C-1	6.69322E-02 ±2.14183E-04	6.59873E-02 ±2.11159E-04	6.69322E-02 ±2.14183E-04

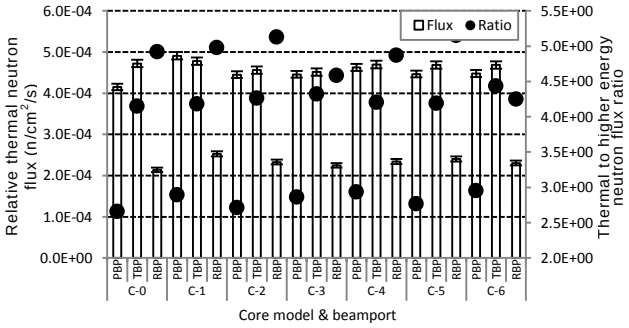

Fig. 6. Relative thermal neutron flux at horizontal beam-ports of the R&R cores.

Neutron flux at lazy susan and vertical irradiation systems

The relative thermal neutron flux and thermal to higher energy neutron flux ratio at the Lazy Susan and vertical irradiation systems (DCT, and PTS) of the R&R cores have been calculated. The findings are presented in Fig. 7. It is seen that the reconfigured core C-1 shows the highest thermal flux at Lazy Susan and DCT compared to that of the reference and other reconfigured cores (Table 4). On the other hand, the reconfigured core C-2 shows the topmost thermal flux at PTS.

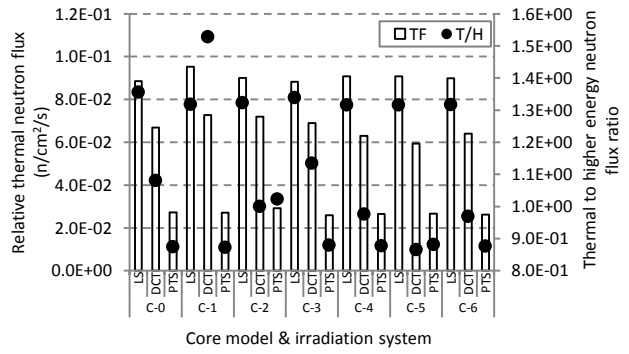

Fig. 7. Relative thermal neutron flux & thermal to higher energy neutron flux ratio at Lazy Susan & vertical beam-ports of the R&R cores.

Photon flux at horizontal beam-ports

It is of great importance to estimate not only the neutron flux but also the photon flux profile in irradiation systems. This is required from an experimental and radiation protection perspective. In this study, the distribution of the relative gamma photon flux of the horizontal beam-ports (piercing, tangential and radial) was calculated with the associated standard deviation. Figure 8 illustrates the relative distribution of gamma photon flux of the horizontal beam-ports of the R&R TRIGA cores. The reconfigured core C-5 and C-6 have approximately the same gamma photon flux reception capability at horizontal beam-ports. The reconfigured core C-5 received the highest gamma photon flux at the piercing and radial beam-port while C-6 at the tangential. In the tangential beam-port the gamma photon flux value of the core C-5 is within the STD limit of the core C-6. It can be concluded that the horizontal beam ports of the reconfigured core C-5 have the best capability for obtaining gamma photon flux.

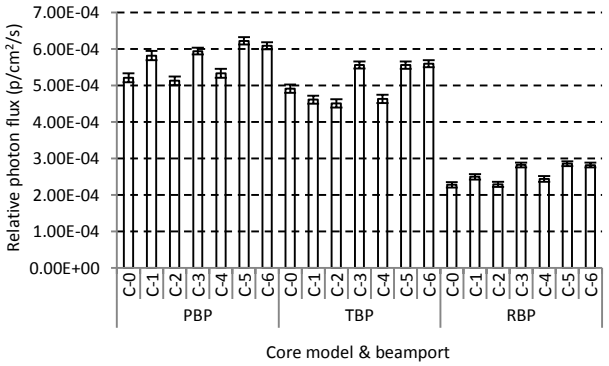

Fig. 8. Relative photon flux at horizontal beam-ports of the R&R cores.

Photon flux at lazy susan and vertical irradiation systems

In this study, the relative distribution of gamma photon flux in Lazy Susan and axial beam-ports (DCT and PTS) was calculated using the associated standard deviation. Figure 9 demonstrates the relative gamma photon flux of Lazy Susan and axial beam-ports of the R&R TRIGA cores. The reconfigured core C-1 received the highest gamma photon flux at the Lazy Susan. Reconfigured cores C-2 and C-4 have approximately the same gamma photon flux reception capacity at axial beam ports. In the DCT and PTS, the reference core (C-0) and the reconfigured core C-2 received the highest gamma photon flux.

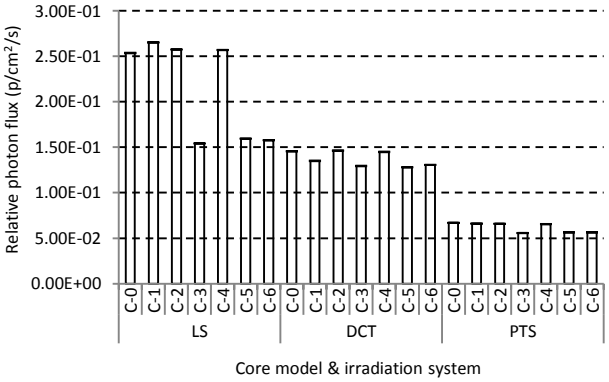

Fig. 9. Relative photon flux at Lazy Susan & vertical beam-ports of the R&R cores.

Axial flux at vertical irradiation systems

In order to irradiate a sample with a fixed dose, it is therefore very important to know the comparative flux at different axial points of vertical irradiation systems (DCT, PTS). In this study, the relative axial flux of DCT and PTS has been calculated at different vertical distances. The vertical distance of the core is divided into ten equal segments of 16 cm thickness. Total flux is calculated at each axial node (joining point of two segments). The results are displayed in Fig 10. Here, axial node '0' means center, '+' means upper portion and '-' means lower portion, of the core. The reconfigured core C-6 represents the optimum relative axial flux at each axial node of the DCT compared to that of the reference and other reconfigured cores. This is due to the presence of small number of GDEs around the DCT. The reconfigured cores C-3, C-4, and C-5 have the approximately same relative axial flux at the DCT. However, the relative axial flux at each axial node of PTS of all the R&R cores shows approximately the same value.

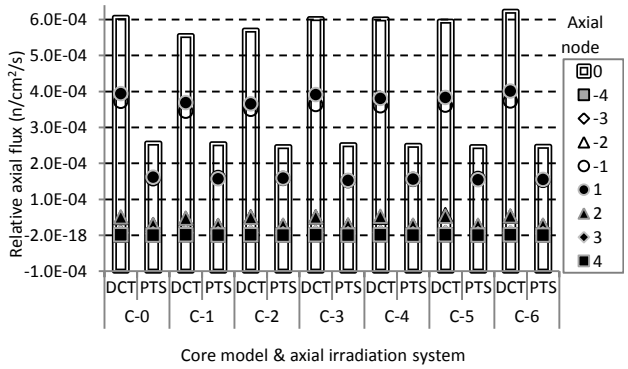

Fig. 10. Relative axial flux at vertical irradiation systems of the R&R cores.

CONCLUSION

Some final remarks can be made on the basis of what has hitherto been observed in this study. In the core criticality calculations, the reconfigured core C-1 displayed the lowest excess reactivity, the highest sub-criticality and thermal flux in the critical state. Moreover, it provided the maximum thermal neutron flux to all the horizontal beam ports, Lazy Susan, and DCT. In addition, it exhibited the highest gamma photon flux at Lazy Susan. On the other hand, the reconfigured core C-5 showed the highest gamma photon flux in radial irradiation systems relative to the other R&R cores (Table 4). Lastly, one can say with certainty that the reconfigured core C-1 is the optimum configuration and comparatively better than the reference core based on the neutronic and photonic performances in the irradiation systems.

AUTHOR CONTRIBUTION

S. M. Shauddin contributed as the only one contributor of this paper. The author read and approved the final version of the paper.

REFERENCES

1. M. S. Islam, M. M. Haque, M. A. Salam *et al.*, *Operation Experience with the 3 MW TRIGA Mark-II Research Reactor of Bangladesh,* World TRIGA Users Conference, Vienna (2004) 47.
2. A. Kolšek, V. Radulović and L. Snoj, *Using TRIGA Mark-II Research Reactor for Irradiation with Thermal Neutrons*, Proceedings of the International Conference Nuclear Energy for New Europe (2013) 614.
3. D. Fourmentel, J-F. Villard, A. Lyoussi *et al.*, *Combined analysis of neutron and photon flux measurements for the Jules Horowitz Reactor core mapping*, Proceedings of the Conference: ANIMMA (2011) 6172905.
4. D. Chiesa, M. Carta, V. Fabrizio *et al.*, Eur. Phys. J. Plus (2020) 135:349.
5. M. A. A. Rosdi, P. S. Goh, F. Idris *et al.*, *Neutron and Gamma Ray Fluencies Measurement at Radial Beam Port 1 of TRIGA MARK II PUSPATI Research Reactor,* IOP Conf. Ser.: Mater. Sci. Eng. 298 (2018) 012033.
6. M. Albarqi, R. Alsulami, T. Akyurek *et al.*, J. Radioanal. Nucl. Chem. **321**(2019) 109.
7. S. Shalbi, W. Norhayati, W. Salleh *et al.*, *Neutron Measurement at the Thermal Column of the Malaysian Triga Mark II Reactor using Gold Foil Activation Method and TLD*, IOP Conf. Ser.: Mater. Sci. Eng. **298** (2018) 012031.
8. S. M. Shauddin, Ann. Nucl. Energy **162** (2021) 108499.
9. Anonymous, X-5 Monte Carlo Team, *MCNP – A General Monte Carlo N-Particle Transport Code*, Version 5, LA-UR-03-1987 (2005) https://rsicc.ornl.gov/codes/ccc/ccc8/ccc-810.html
10. M. B. Chadwick, P. Obložinský, M. Herman *et al.*, Nuclear Data Sheets 107 (2006) 2931.
11. Anonymous, X-5 Monte Carlo Team, *MCNP - A General Monte Carlo N-Particle Transport Code*, Version 5, Vol. I: User's Guide, LA-UR-03-1987 (2003) https://rsicc.ornl.gov/codes/ccc/ccc8/ccc-810.html
12. R. Yasmeen and M. S. Mahmood, Ann. Nucl. Energy **91** (2016) 2